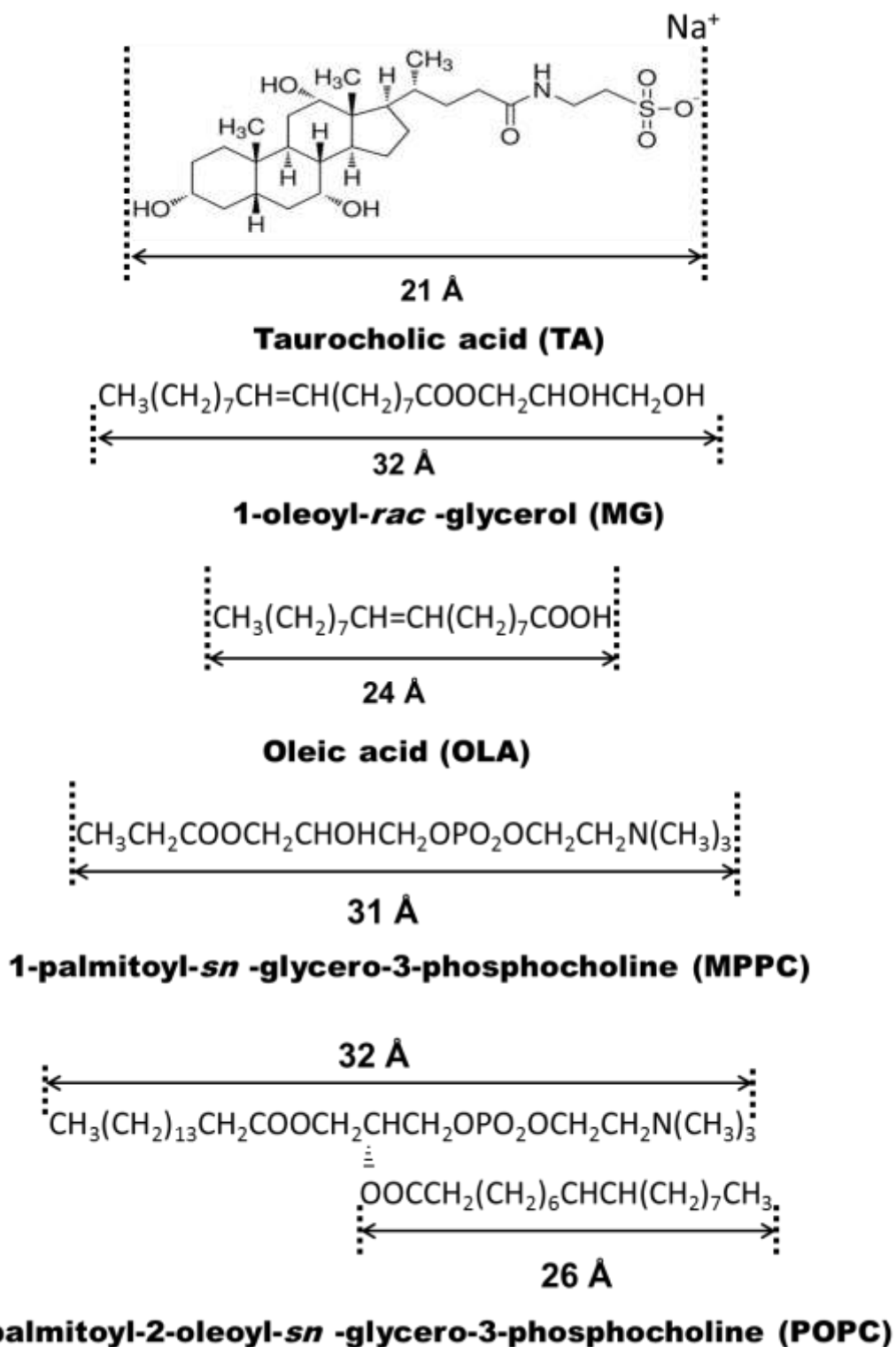# Supporting information

Effects of a lysophosphatidylcholine and a phosphatidylcholine on the morphology of taurocholic acid-based mixed micelles as determined by small-angle X-ray scattering

Hideki Aizawa, Sosaku Ichikawa, Eiichi Kotake-Nara, and Akihiko Nagao

S1. Molecular structures

Taurocholic acid (TA) — 21 Å

$CH_3(CH_2)_7CH=CH(CH_2)_7COOCH_2CHOHCH_2OH$ — 32 Å

1-oleoyl-*rac*-glycerol (MG)

$CH_3(CH_2)_7CH=CH(CH_2)_7COOH$ — 24 Å

Oleic acid (OLA)

$CH_3CH_2COOCH_2CHOHCH_2OPO_2OCH_2CH_2N(CH_3)_3$ — 31 Å

1-palmitoyl-*sn*-glycero-3-phosphocholine (MPPC)

32 Å
$CH_3(CH_2)_{13}CH_2COOCH_2CHCH_2OPO_2OCH_2CH_2N(CH_3)_3$
$OOCCH_2(CH_2)_6CHCH(CH_2)_7CH_3$ — 26 Å

1-palmitoyl-2-oleoyl-*sn*-glycero-3-phosphocholine (POPC)

Figure S1 Molecular structures of taurocholic acid, 1-oleoyl-*rac*-glycerol, oleic acid, 1-palmitoyl-*sn*-glycero-3-phosphocholine, and 1-palmitoyl-2-oleoyl-*sn*-glycero-3-phosphocholine. The length of each molecule was obtained by using GaussView 5 graphical interface software.

2
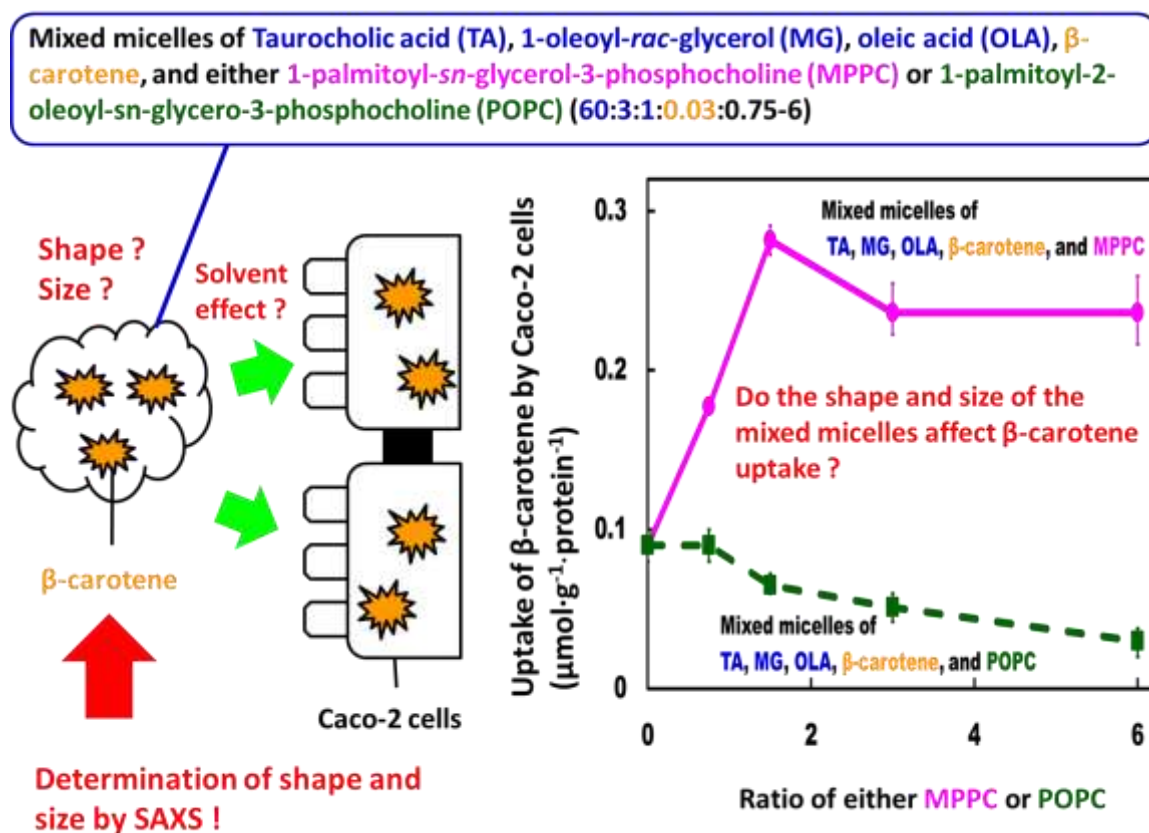
Figure S2 Study outline and graph of β-carotene uptake by Caco-2 cells against the ratio of either MPPC or POPC in micelles of TA, MG, OLA, β-carotene, and either MPPC or POPC (60:3:1:0.03:0.75–6). The graph shows β-carotene uptake by Caco-2 cells against the ratio of either MPPC (magenta circles and solid line) or POPC (green rectangles and dashed line) in mixed micelles of TA, MG, OLA, β-carotene, and either MPPC or POPC. All values for β-carotene uptake were taken, with permission, from Figure 1 of Sugawara *et al.* (2001). *J. Nutr.* 131 (2001) 2921.

Table S1   Micelle mixture molar ratios and total concentrations (Total concn) of taurocholic acid (TA), 1-oleoyl-*rac*-glycerol (MG), oleic acid (OLA), β-carotene,1-palmitoyl-*sn*-glycero-3-phosphocholine (MPPC), and 1-palmitoyl-2-oleoyl-*sn*-glycero-3-phosphocholine (POPC) relative to β-carotene uptake by Caco-2 cells.

Micelle mixture molar ratio of TA:MG:OLA:β-carotene:MPPC:POPC	Total concn		β-carotene uptake by Caco-2 cells[a]
	(mM)	(wt %)	(μmol·g^{-1}·protein^{-1})
60:3:1:0.03:0:0	2.13	0.112	0.10
60:3:1:0.03:0.75:0	2.16	0.113	0.18
60:3:1:0.03:1.5:0	2.18	0.115	0.29
60:3:1:0.03:3:0	2.23	0.117	0.23
60:3:1:0.03:6:0	2.33	0.122	0.23
60:3:1:0.03:0:0.75	2.16	0.114	0.095
60:3:1:0.03:0:1.5	2.18	0.116	0.063
60:3:1:0.03:0:3	2.23	0.120	0.053
60:3:1:0.03:0:6	2.33	0.127	0.026

[a]The β-carotene uptake values in this table were taken with permission from Figure 1 of Sugawara *et al.* (2001). *J. Nutr*. 131 (2001) 2921.

S3. Methods for analyzing small-angle X-ray scattering data

S3.1. Data treatment

The measured X-ray intensity, I$(q)^m$ (arbitrary units), obtained by integrating around Debye-Scherrer rings on the two-dimensional image of the small-angle X-ray scattering (SAXS) data, and the scattering vectors, q (in Å^{-1}), were calculated as follows: $q = (4\pi/\lambda) \sin \theta$, where π, λ, and 2θ are the circular constant, wavelength of the X-rays, and scattering angle, respectively, by using Fit-2D software and the standard spreadsheet application Microsoft Excel[31–32]. Recently, units of nm^{-1} have been used for q; however, because Å is more commonly used for the atomic distances, we used Å^{-1} for q to avoid possible unit conversion errors.

X-ray intensity at q, I$(q)'$, divided by time, t (in seconds), is given by [33, 34]

$$\frac{I(q)'}{t} = \frac{I_0}{t} \eta S D_t \frac{A}{L_2^2} T \frac{d\Sigma}{d\Omega}(q) \tag{S1}$$

where I_0 is the entering intensity for time; η is the sensitivity of the detector; S is a cross-section of the X-ray; D_t is the thickness of the sample; A is an image pixel area of the detector, that is, a minimum area of image detection; L is the distance from the sample to the detector; T is the transmission of the sample; $\frac{d\Sigma}{d\Omega}(q)$ is a differential scattering cross-section per unit volume (*i.e.*, DSCS(q)).

Really I$(q)^m$ was measured X-ray intensity absorbed by the sample and elastic scattered from the sample; therefore, I$(q)^m$ needed to be corrected to measured X-ray intensity elastic scattered from the sample, I$(q)^{m'}$, because small-angle X-ray scattering is assumed an elastic scattering of X-rays.

Because of the need to correct I$(q)^{m'}$, the value for the ionization chamber in front of the cuvette holder to which a full cuvette of sample was attached, given in amperes, $I_{0,sample}$; and the value for the ionization chamber at the back of the cuvette holder to which a full cuvette of sample was attached, given in amperes, $I_{1,sample}$; and the value for ionization chamber, which measured the background radiation, in front of the empty cuvette holder, given in amperes, $I_{0,BG}$; and the value for ionization chamber, which measured the background radiation, at the back of the empty cuvette holder, given in amperes, $I_{1,BG}$, were used. The measured quantity of transmission for a full cuvette of sample, T^m_{sample}, is determined from $I_{0,sample}$, $I_{1,sample}$, $I_{0,BG}$, and $I_{1,BG}$.

$$T^m_{sample} = \frac{\frac{I_{1,sample}}{t} - \frac{I_{1,BG}}{t}}{\frac{I_{0,sample}}{t} - \frac{I_{0,BG}}{t}} \tag{S2}$$

$$I(q)^{m'} = \frac{I(q)^m}{T^m_{sample}} \tag{S3}$$

The 2.5-GeV electron storage Photon Factory ring in the High Energy Accelerator Research Organization (Tsukuba, Japan) provided the synchrotron radiation by switching the storage ring operation mode or top-up storage ring operation mode to maintain, investigate, or improve the accelerator instruments. The mode changed depending on the day. On days when the storage ring operation mode was used, the ring current and measured quantity of the entering X-ray intensity, I_0^m, exponentially decreased over time with the loss of electrons.

On days when the top-up storage ring operation mode was used, the ring current and I_0^m were kept nearly constant by injecting electrons at short intervals to compensate for the loss of electrons. The ring current and I_0^m varied by several percentage points over time; therefore, I_0^m needed to be corrected.

Because of the need to correct I_0^m, the value for the ionization chamber in front of the empty cuvette holder, given in amperes, $I_{0,ECH}$; and $I_{0,sample}$, and $I_{0,BG}$, were used. The empty cuvette holder is air in the space between the ionization chamber in front of the empty cuvette holder and the ionization chamber at the back of the empty cuvette holder.

$$I_0 = I_0^m \frac{\frac{I_{0,ECH}}{t} - \frac{I_{0,BG}}{t}}{\frac{I_{0,sample}}{t} - \frac{I_{0,BG}}{t}} \tag{S4}$$

$$I(q)^{m''} = I(q)^{m'} \frac{\frac{I_{0,ECH}}{t} - \frac{I_{0,BG}}{t}}{\frac{I_{0,sample}}{t} - \frac{I_{0,BG}}{t}} \tag{S5}$$

Because the square imaging plate detector was installed at a 90° angle to the entering X-ray and because the distances from the cuvette to the detector differed at scattering angles, the measured quantity of X-ray intensity scattered from the sample, $I(q)^{m'}$, was angle dependent. $I(q)^{m'}$ must be corrected depending on the distance and intensity of the X-rays at the distance from the cuvette to the detector, L, and the 0° scattering angle. We assumed that as the distance from the sample to the detector becomes longer and longer, the angle-dependent X-ray intensity would fluctuate although it is normally ignored. The X-ray intensity scattered from the sample decreases in inverse proportion to the square of the distance from the sample to the detector[35].

$$I(q)' = I(q)^{m''} \frac{64\pi^4}{q^4\lambda^4 - 16q^2\lambda^2\pi^2 + 64\pi^4} \tag{S6}$$

X-ray intensity at q per time, $I(q)$, is given by

$$I(q) = I(q)^{mc} = \frac{I(q)'}{t} = \frac{I_0}{t}\eta S D_t \frac{A}{L_2^2} T \frac{d\Sigma}{d\Omega}(q) \tag{S7}$$

From another viewpoint, equation (S7) can be solved based on the sample and experimental conditions used. It consists of transmissions and intensities for measured sample components (see Figure S2). The

basic concepts behind the equations have been described in the literature[33]. Differences in the solutions to the equations in the literature and those described here depend on whether or not transmission data and intensities for components of the sample solution and the air in the space between the ionization chamber in front of the empty cuvette holder and the ionization chamber at the back of the empty cuvette holder have been added. The literature equations do not take into account differences in transmission between the solute and the solvent in the sample solution and the air in the space between the ionization chamber in front of the empty cuvette holder and the ionization chamber at the back of the empty cuvette holder even though a difference is supposed to exist.

The measured quantity of transmission, T^{m}, is determined from the value for the ionization chamber in front of the cuvette holder, I_0, and the value for the ionization chamber behind the cuvette holder, I_1 (see Figure S2). Moreover, T^{m} is determined by the sample and experimental conditions used; it consists of the transmission data for the measured sample components.

Transmissions of measured samples are given by

$$T_{\mathrm{holder}}^{\mathrm{m}} = T_{\mathrm{holder}} = \frac{\frac{I_{1,\mathrm{holder}}}{t} - \frac{I_{1,\mathrm{BG}}}{t}}{\frac{I_{0,\mathrm{holder}}}{t} - \frac{I_{0,\mathrm{BG}}}{t}} \tag{S8}$$

$$T_{\mathrm{cuvette}}^{\mathrm{m}} = T_{\mathrm{cuvette}} T_{\mathrm{holder}} = \frac{\frac{I_{1,\mathrm{cuvette}}}{t} - \frac{I_{1,\mathrm{BG}}}{t}}{\frac{I_{0,\mathrm{cuvette}}}{t} - \frac{I_{0,\mathrm{BG}}}{t}} \tag{S9}$$

$$T_{\mathrm{solvent}}^{\mathrm{m}} = T_{\mathrm{solvent}} T_{\mathrm{cuvette}} T_{\mathrm{holder}} = \frac{\frac{I_{1,\mathrm{solvent}}}{t} - \frac{I_{1,\mathrm{BG}}}{t}}{\frac{I_{0,\mathrm{solvent}}}{t} - \frac{I_{0,\mathrm{BG}}}{t}} \tag{S10}$$

$$T_{\mathrm{solution}}^{\mathrm{m}} = T_{\mathrm{solute}} T_{\mathrm{solvent}} T_{\mathrm{cuvette}} T_{\mathrm{holder}} = \frac{\frac{I_{1,\mathrm{solute}}}{t} - \frac{I_{1,\mathrm{BG}}}{t}}{\frac{I_{0,\mathrm{solute}}}{t} - \frac{I_{0,\mathrm{BG}}}{t}} \tag{S11}$$
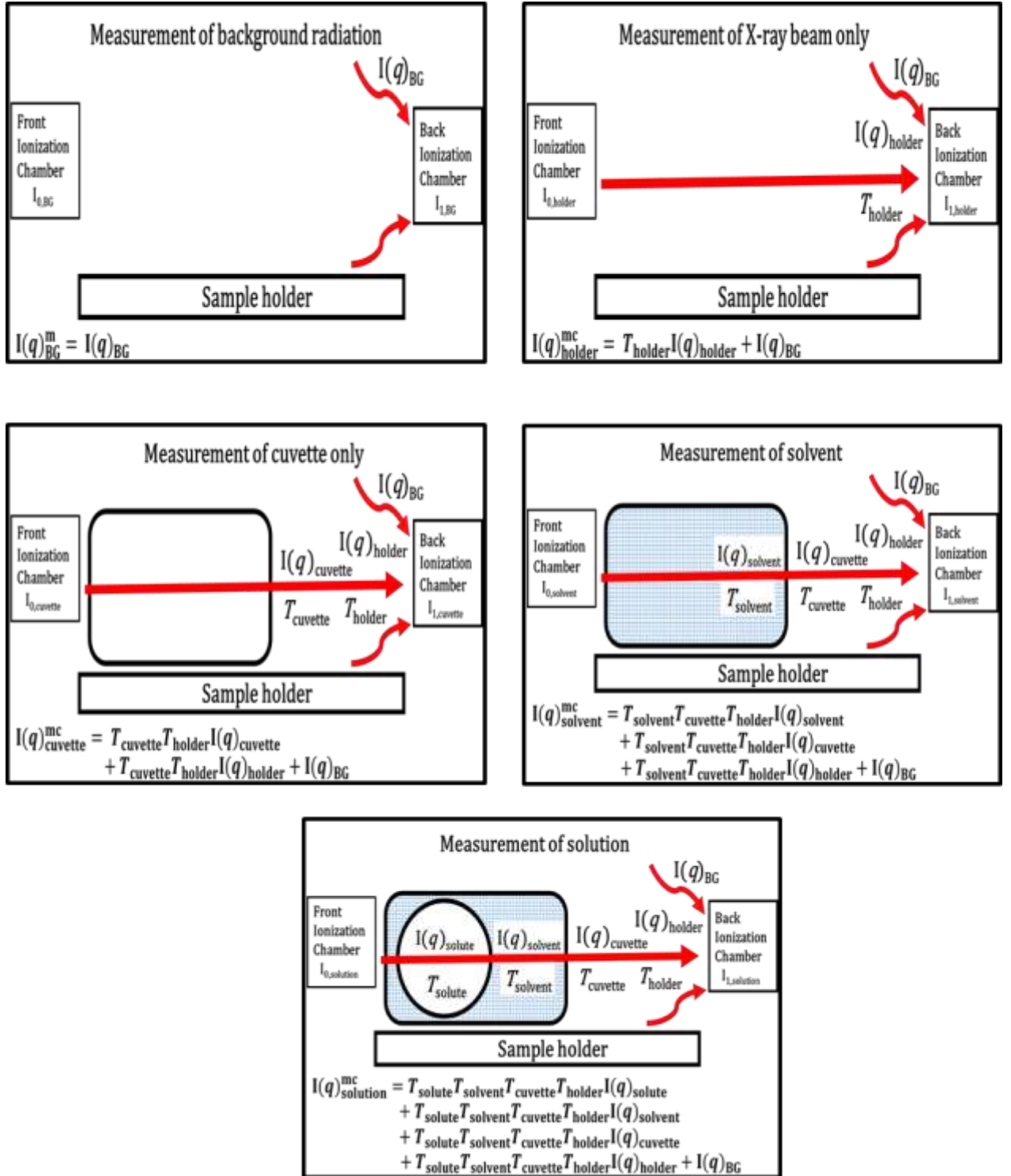
The intensity of the components of the solvent is given by

$$\mathrm{I}(q)_{\mathrm{solvent}} = \frac{\mathrm{I}(q)_{\mathrm{solvent}}^{\mathrm{mc}}}{T_{\mathrm{solvent}}^{\mathrm{m}}} - \frac{\mathrm{I}(q)_{\mathrm{cuvette}}^{\mathrm{mc}}}{T_{\mathrm{cuvette}}^{\mathrm{m}}} + \frac{\mathrm{I}(q)_{\mathrm{BG}}^{\mathrm{m}}}{T_{\mathrm{cuvette}}^{\mathrm{m}}} - \frac{\mathrm{I}(q)_{\mathrm{BG}}^{\mathrm{m}}}{T_{\mathrm{solvent}}^{\mathrm{m}}} \tag{S12}$$

The intensity for water is given by

$$\mathrm{I}(q)_{\mathrm{water}} = \frac{\mathrm{I}(q)_{\mathrm{water}}^{\mathrm{mc}}}{T_{\mathrm{water}}^{\mathrm{m}}} - \frac{\mathrm{I}(q)_{\mathrm{cuvette}}^{\mathrm{mc}}}{T_{\mathrm{cuvette}}^{\mathrm{m}}} + \frac{\mathrm{I}(q)_{\mathrm{BG}}^{\mathrm{m}}}{T_{\mathrm{cuvette}}^{\mathrm{m}}} - \frac{\mathrm{I}(q)_{\mathrm{BG}}^{\mathrm{m}}}{T_{\mathrm{solvent}}^{\mathrm{m}}} \tag{S13}$$

Accordingly, the intensity for the solute is given by

$$\mathrm{I}(q)_{\mathrm{solute}} = \frac{\mathrm{I}(q)_{\mathrm{solution}}^{\mathrm{mc}}}{\mathrm{T}_{\mathrm{solution}}^{\mathrm{m}}} - \frac{\mathrm{I}(q)_{\mathrm{solvent}}^{\mathrm{mc}}}{\mathrm{T}_{\mathrm{solvent}}^{\mathrm{m}}} + \frac{\mathrm{I}(q)_{\mathrm{BG}}^{\mathrm{m}}}{\mathrm{T}_{\mathrm{cuvette}}^{\mathrm{m}}} - \frac{\mathrm{I}(q)_{\mathrm{BG}}^{\mathrm{m}}}{\mathrm{T}_{\mathrm{solution}}^{\mathrm{m}}} \tag{S14}$$

Measurement of background radiation

$I(q)_{BG}$

Front Ionization Chamber $I_{0,BG}$

Back Ionization Chamber $I_{1,BG}$

Sample holder

$$I(q)_{BG}^{m} = I(q)_{BG}$$

Measurement of X-ray beam only

$I(q)_{BG}$

Front Ionization Chamber $I_{0,holder}$

$I(q)_{holder}$

T_{holder}

Back Ionization Chamber $I_{1,holder}$

Sample holder

$$I(q)_{holder}^{mc} = T_{holder}I(q)_{holder} + I(q)_{BG}$$

Measurement of cuvette only

$I(q)_{BG}$

Front Ionization Chamber $I_{0,cuvette}$

$I(q)_{cuvette}$ $I(q)_{holder}$

$T_{cuvette}$ T_{holder}

Back Ionization Chamber $I_{1,cuvette}$

Sample holder

$$I(q)_{cuvette}^{mc} = T_{cuvette}T_{holder}I(q)_{cuvette}$$
$$+ T_{cuvette}T_{holder}I(q)_{holder} + I(q)_{BG}$$

Measurement of solvent

$I(q)_{BG}$

Front Ionization Chamber $I_{0,solvent}$

$I(q)_{solvent}$ $I(q)_{cuvette}$ $I(q)_{holder}$

$T_{solvent}$ $T_{cuvette}$ T_{holder}

Back Ionization Chamber $I_{1,solvent}$

Sample holder

$$I(q)_{solvent}^{mc} = T_{solvent}T_{cuvette}T_{holder}I(q)_{solvent}$$
$$+ T_{solvent}T_{cuvette}T_{holder}I(q)_{cuvette}$$
$$+ T_{solvent}T_{cuvette}T_{holder}I(q)_{holder} + I(q)_{BG}$$

Measurement of solution

$I(q)_{BG}$

Front Ionization Chamber $I_{0,solution}$

$I(q)_{solute}$ $I(q)_{solvent}$ $I(q)_{cuvette}$ $I(q)_{holder}$

T_{solute} $T_{solvent}$ $T_{cuvette}$ T_{holder}

Back Ionization Chamber $I_{1,solution}$

Sample holder

$$I(q)_{solution}^{mc} = T_{solute}T_{solvent}T_{cuvette}T_{holder}I(q)_{solute}$$
$$+ T_{solute}T_{solvent}T_{cuvette}T_{holder}I(q)_{solvent}$$
$$+ T_{solute}T_{solvent}T_{cuvette}T_{holder}I(q)_{cuvette}$$
$$+ T_{solute}T_{solvent}T_{cuvette}T_{holder}I(q)_{holder} + I(q)_{BG}$$

Figure S3 Basic concepts behind the equations for $I(q)^{mc}$. $I(q)_{BG}$, $I(q)_{holder}$, $I(q)_{cuvette}$, $I(q)_{solvent}$, and $I(q)_{solute}$ are the intensities for the components of the background radiation, cuvette holder, cuvette, solvent, and solute, respectively. T_{holder}, $T_{cuvette}$, $T_{solvent}$, and T_{solute} are the transmissions for the components of the cuvette holder, cuvette, solvent, and solute, respectively.

In the literature[33], the intensity of the solute was determined by subtracting the intensity of the solvent from the intensity of the solution. The intensity of water was determined by subtracting the intensity of an empty cuvette from the intensity of a full cuvette of water. The reason for these calculations do not take into account the difference in transmission between the solute and the solvent in the sample solution or the air in the space between the ionization chamber in front of the empty cuvette holder and the ionization chamber at the back of the empty cuvette holder. However, because equations S13 and S14 take these differences into account, these subtraction calculations are not necessary.

The measured and corrected X-ray intensity at q divided by time for the empty holder (*i.e.*, without attaching the cuvette to the cuvette holder), $I(q)_{holder}^{mc}$, that is, the X-ray beam alone, is shown in Figure S3. The intensity rapidly decreased in the q range of 0 to 0.0977. This rapid decrease was likely caused by a corona of intense X-rays that surrounds the beamstop as a result of scattering by the beamstop like the corona of the sun when watching a solar eclipse. Because we assumed that we could not reliably measure the intensity of the X-rays scattered by the sample by measuring the intensity of the X-rays scattered by the beamstop in the q range of 0 to 0.0977, we deleted the X-ray intensity data in this range. The intensity decreased non-linearly for q values of 0.3432 and greater. Because we felt that we could not reliably measure the intensity of the X-rays scattered by the sample in the q range of 0.3432 and above, we discarded the X-ray intensity data in this range. As result, the active q range of 0.0977 to 0.3432 was calibrated.
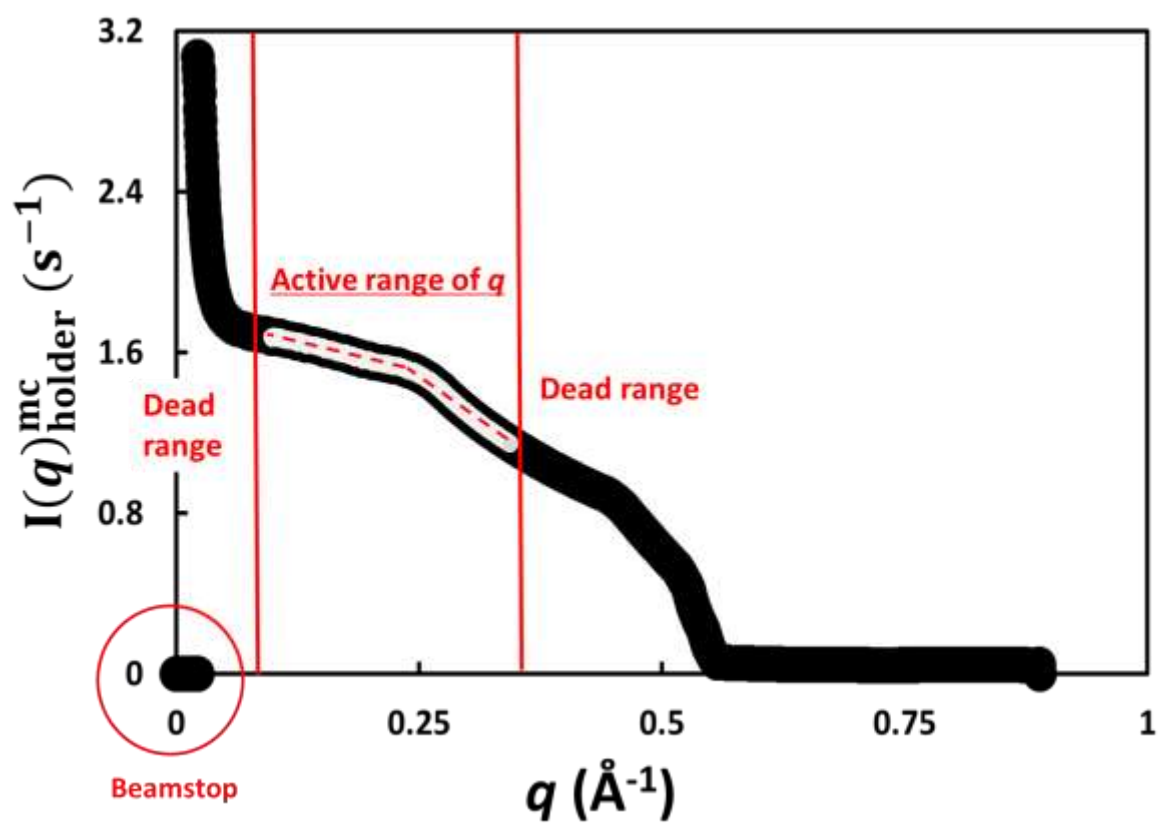
Figure S4 Graph of measured X-ray intensity at scattering vectors, q, divided by time, $\mathrm{I}(q)_{\mathrm{holder}}^{\mathrm{mc}}$, against q for the empty holder (*i.e.*, without attaching the cuvette to the cuvette holder). The black line and the red dashed line represent the scattering data and the active range of q, respectively.

The graph of intensity at q divided by time calculated from equation (S10), $I(q)_{water}$, against q for water shows a proportionately decreasing diagonal line (Figure S4). The value of $I(q)_{water}$–intercept, $I(0)_{water}$, at 293 K is equal to differential scattering cross-sections of water, $\frac{d\Sigma}{d\Omega}(0)_{water}$, 164 [in p (pico-) Å^{-1}], that is $(I(0)_{water}$–intercept value$) = \frac{d\Sigma}{d\Omega}(0)_{water} = 164$ pÅ^{-1} [36].

If the same SAXS equipment is used, differential scattering cross-sections of solute, $\frac{d\Sigma}{d\Omega}(q)_{solute}$ can be calculated by using the following equation:

$$\frac{I(q)_{solute}}{I(0)_{water}} = \frac{\frac{I_0}{t}\eta S D_{t,solute}\frac{A}{L_2^2}T_{solute}\frac{d\Sigma}{d\Omega}(q)_{solute}}{\frac{I_0}{t}\eta S D_{t,water}\frac{A}{L_2^2}T_{water}\frac{d\Sigma}{d\Omega}(0)_{water}} \tag{S15}$$

$$\frac{d\Sigma}{d\Omega}(q)_{solute} = \frac{I(q)_{solute}D_{t,water}T_{water}\frac{d\Sigma}{d\Omega}(0)_{water}}{I(0)_{water}D_{t,solute}T_{solute}} \tag{S16}$$

where $D_{t,\,solute}$ is the thickness of a cuvette full of sample solution; $D_{t,\,water}$ is the thickness of a cuvette full of water.
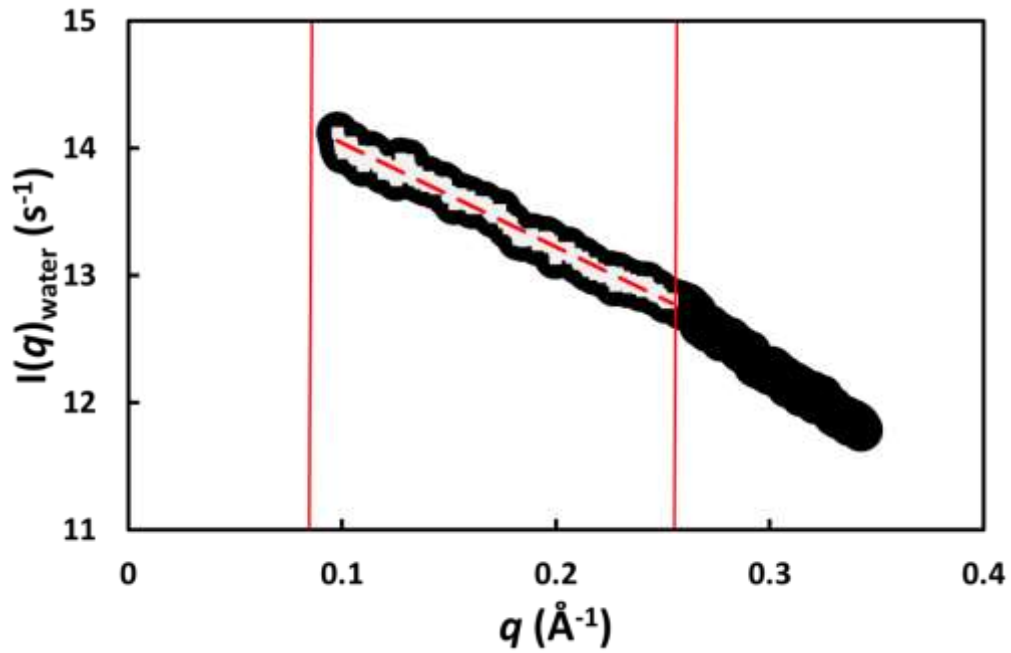
Figure S5 Graph of intensity at scattering vectors, q, divided by time calculated from equation (S13), $I(q)_{water}$, against q for water. The black line and the red dashed line represent scattering data and the proportionately decreasing diagonal line used to calculate the value of $I(q)_{water}$–intercept, $I(0)_{water}$, respectively.

S3.2. Method for a least-squares fit of the model to the SAXS data

We attempted to fit the SAXS data to each of various alternative models. Least-squares fit calculations indicated that the core–shell sphere model provided the best fit for the SAXS data for micelles of taurocholic acid (TA) in phosphate-buffered saline (PBS) or Dulbecco's modified Eagle medium (DMEM) and for mixed micelles of TA, 1-oleoyl-*rac*-glycerol (MG), and oleic acid (OLA) (60:3:1) in PBS or DMEM. The core–shell oblate ellipsoid model provided the best fit for mixed micelles of TA, MG, OLA, and 1-palmitoyl-*sn*-glycero-3-phosphocholine (MPPC) (60:3:1:0.03:0.75–12) and mixed micelles of TA, MG, OLA, and 1-palmitoyl-2-oleoyl-*sn*-glycero-3-phosphocholine (POPC) (60:3:1:0.03:0.75–6) in PBS or DMEM. The core–shell cylinder model provided the best fit for mixed micelles of TA, MG, OLA, and POPC (60:3:1:0.03:9–12) in PBS or DMEM.

Geometric shapes for core–shell spheres, core–shell oblate ellipsoids, and core–shell cylinders are shown in Figure S5.
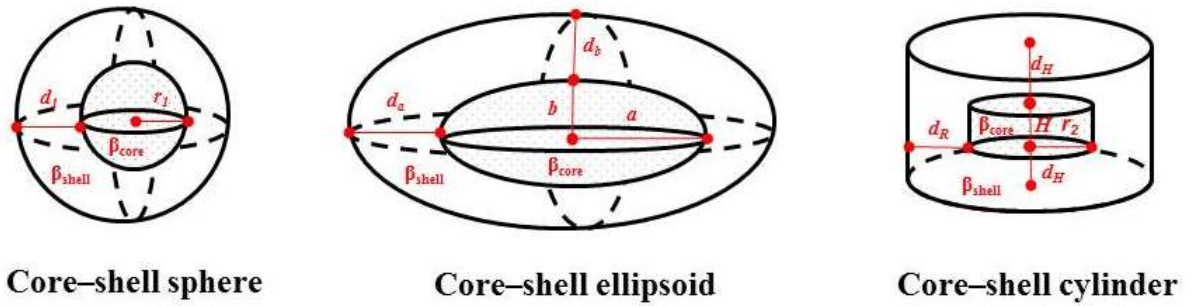
Figure S6 Geometric shapes for core–shell spheres, core–shell oblate ellipsoids, and core–shell cylinders.

The mathematical descriptions of the core–shell sphere, the core–shell ellipsoid, and the core–shell cylinder models have been reported elsewhere [22-26,33,37]; however, they are given below because they are important for this study.

DSCS(q)$_{\text{solute}}$ is given by

$$\text{DSCS}(q)_{\text{solute}} = nV_{\text{solute}}^2\Delta\beta^2 F(q)^2 S(q) \tag{S17}$$

where n, V_{solute}, and $\Delta\beta$ are the number density of a solute particle, the volume of the solute particle, and the difference in scattering length density between the solute particles and the solvent or matrix, respectively; $F(q)$ and $S(q)$ are the form factor and structure factor, respectively. The form factor describes the structure of the solute particle; the structure factor describes the interference of scattering from different solute particles and contains information about the interaction between the solute

particles[33,36]. It is easy for the structure factor to affect complex systems and concentrated solute particle solutions.

The procedure to fit the model to the data is described below.

Step 1: The shape and size of the solute are first determined by a least-squares fit of the SAXS data to equation (S18) described below, that is equation (S17) removed S(q)

$$\text{DSCS}(q)_{\text{solute}} = nV_{\text{solute}}^2 \Delta\beta^2 F(q)^2 \qquad \text{(S18)}$$

Step 2: The experimental structure factor, S(q)$_{\text{experiment}}$, is determined by equation (S19):

$$S(q)_{\text{experiment}} = \frac{\text{DSCS}(q)_{\text{solute,experiment}}}{\text{DSCS}(q)_{\text{solute,equation(S18)}}} \qquad \text{(S19)}$$

where DSCS(q)$_{\text{solute, experiment}}$ is the scattering cross-section calculated from equation (S16) on the basis of the SAXS data and DSCS(q)$_{\text{solute, equation (S18)}}$ is the scattering cross-section calculated from equation (S18).

Step 3: S(q)$_{\text{experiment}}$ is determined by a least-squares fit of S(q)$_{\text{experiment}}$ to the ideal S(q) equations on the basis of various assumptions about the shape and size of the solute and whether or not the interface of the solute has a positive or negative charge, etc. [33,37]. If the particles of the solute in sample solution do not interact with each other, S(q) = 1; that is, S(q)$_{\text{experiment}}$ = 1 must be shown. If the particles of the solute in the sample solution do not interact with each other, the least-squares fit of S(q)$_{\text{experiment}}$ to the ideal S(q) equations is not needed.

Step 4: DSCS(q)$_{\text{solute}}$ is determined by a least-squares fit of the SAXS data to equation (S17) substituting the result of Step 1 to 3 of 4 to finely adjust.

For the core–shell sphere, V_{solute} and $\Delta\beta^2 F(q)^2$ are given by

$$V_{\text{solute}} = \frac{4}{3}\pi(r_1 + d_1)^3 \qquad \text{(S20)}$$

and

$$\Delta\beta^2 F(q)^2 = \left[\frac{FSP(q)_1 + FSP(q)_2}{FSP(\text{q})_3}\right]^2 \qquad \text{(S21)}$$

where

$$FSP(q)_1 = (\beta_{\text{core}} - \beta_{\text{shell}})V_{\text{core}}FS(q, r_1) \qquad \text{(S22)}$$

and

$$V_{\text{core}} = \frac{4}{3}\pi r_1^3 \qquad \text{(S23)}$$

and

13

$$F(q, R_f) = \frac{3\sin(q \cdot R_f) - 3(q \cdot R_f)\cos(q \cdot R_f)}{(q \cdot R_f)^3} \tag{S24}$$

and

$$FSP(q)_2 = (\beta_{shell} - \beta_{solvent})V_{solute}FS[q, (r_1 + d_1)] \tag{S25}$$

and

$$FSP(q)_3 = (\beta_{core} - \beta_{shell})V_{core} + (\beta_{shell} - \beta_{solvent})V_{solute} \tag{S26}$$

where r_1 and β_{core} are the radius of the sphere and the scattering length density of the core, respectively; d_1 and β_{shell} are the length and the scattering length density of the shell, respectively; and $\beta_{solvent}$ is the scattering length density of the solvent.

Five parameters (n, r_1, d_1, β_{core}, and β_{shell}) for equation (S18) and equations (S20) to (S26) were determined by a least-squares fit of the SAXS data to the model. Values of β_{core} and β_{shell} were roughly estimated, and the exact value of $\beta_{solvent}$ was determined from the density and number of electrons of the molecules in the mixed micelles and the solvents [22-26,33]; that is, β_{core} is given by ($\rho_{core} Ne_{core} r_e N_A)/M_{core}$, where ρ_{core} is the density of the core, Ne_{core} is the electron number of the core molecule, r_e is the classical electron radius, and M_{core} is the molecular weight of the core. β_{shell} is given by ($\rho_{shell} Ne_{shell} r_e N_A)/M_{shell}$, where ρ_{shell} is the density of the shell, Ne_{shell} is the electron number of the shell molecule, and M_{shell} is the molecular weight of the shell. $\beta_{solvent}$ is given by ($\rho_{solvent} Ne_{solvent} r_e N_A)/M_{solvent}$, where $\rho_{solvent}$ is the density of the solvent, Ne_{shell} is the electron number of the solvent molecule, and $M_{solvent}$ is the molecular weight of the solvent.

For the core–shell oblate ellipsoids, V_{solute} and $\Delta\beta^2 F(q)^2$ are given by

$$V_{solute} = \frac{4}{3}\pi(a + d_a)^2(b + d_b) \tag{S27}$$

and

$$\Delta\beta^2 F(q)^2 = \int_0^{\frac{\pi}{2}} \left[\frac{FSP(q)_4 + FSP(q)_5}{FSP(q)_6}\right]^2 \sin x \, dx \tag{S28}$$

and

$$FSP(q)_4 = (\beta_{core} - \beta_{shell})V_{core}FS(q, CSEP_1) \tag{S29}$$

and

$$V_{core} = \frac{4}{3}\pi a^2 b \tag{S30}$$

and

$$CSEP_1 = a\left[\sin^2 x + \left(\frac{b}{a}\right)\cos^2 x\right]^2 \tag{S31}$$

14

and

$$FSP(q)_5 = (\beta_{\text{shell}} - \beta_{\text{solvent}})V_{\text{solute}}FS(q, CSEP_2) \tag{S32}$$

and

$$CSEP_2 = (a + d_a)\left\{\sin^2 x + \left[\frac{(b + d_b)}{(a + d_a)}\right]\cos^2 x\right\} \tag{S33}$$

and

$$FSP(q)_6 = (\beta_{\text{core}} - \beta_{\text{shell}})V_{\text{core}} + (\beta_{\text{shell}} - \beta_{\text{solvent}})V_{\text{solute}} \tag{S34}$$

where a, b, and β_{core} are the x-axis, the y-axis, and the scattering length density of the core, respectively; d_a, d_b, and β_{shell} are the length of the x-axis, the length of the y-axis, and the scattering length density of the shell, respectively; β_{solvent} is the scattering length density of the solvent; and x is distance on the x-axis.

Seven parameters (n, a, b, d_a, d_b, β_{core}, and β_{shell}) for equation (S18) and equations (S27) to (S34) were determined by a least-squares fit of the SAXS data to the model. Values of β_{core} and β_{shell} were roughly estimated, and the exact value of β_{solvent} was determined from the density and the number of electrons of the molecules in the mixed micelles and the solvents[22-26,33]; that is, β_{core}, β_{shell}, and β_{solvent} were calculated from the above equation for β_{core}, β_{shell}, and β_{solvent}.

For the core–shell cylinder, V_{solute} and $\Delta\beta^2 F(q)^2$ are given by

$$V_{\text{solute}} = \pi(r_2 + d_2)^2 H \tag{S35}$$

and

$$\Delta\beta^2 F(q)^2 = \int_0^{\frac{\pi}{2}} \left[\frac{CCF(q)_1 + CCF(q)_2}{CCF(q)_3}\right]^2 \sin x \, dx \tag{S36}$$

where

$$CCF(q)_1 = \frac{2\pi r_2^2 H(\beta_{\text{core}} - \beta_{\text{shell}})J_1(qr_2\sin x)\sin\left(\frac{qH\cos x}{2}\right)}{qr_2\sin x\frac{qH\cos x}{2}} \tag{S37}$$

and

$$CCF(q)_2 = \frac{2\pi(r_2 + d_2)^2(H + 2d_H)(\beta_{\text{shell}} - \beta_{\text{solvent}})J_1[q(r_2 + d_2)\sin x]\sin\left[\frac{q(H + 2d_H)\cos x}{2}\right]}{q(r_2 + d_2)\sin x\frac{q(H + 2d_H)\cos x}{2}} \tag{S38}$$

and

$$CCF(q)_3 = \pi r_2^2 H(\beta_{\text{core}} - \beta_{\text{shell}}) + \pi(r_2 + d_2)^2(H + 2d_H)(\beta_{\text{shell}} - \beta_{\text{solvent}}) \tag{S39}$$

where r_2, H, and β_{core} are the radius of the circular base of the core cylinder, the height of the core, and the scattering length density of the core, respectively; d_2, d_H, and β_{shell} are the length of r_2, the length of H, and the scattering length density of the shell, respectively; $\beta_{solvent}$ is the scattering length density of the solvent; $J_1(x)$ is the first order Bessel function; and x is the distance on the x-axis.

Seven parameters (n, r_2, d_1, H, d_H, β_{core}, and β_{shell}) for equation (S18) and equations (S35) to (S39) were determined by a least-squares fit of the SAXS data to the model. Values of β_{core} and β_{shell} were roughly estimated, and the exact value of $\beta_{solvent}$ was determined from the density and the number of electrons of the molecules in the mixed micelles and the solvent [22-26,33]; that is, β_{core}, β_{shell}, and $\beta_{solvent}$ were calculated from the above equation for β_{core}, β_{shell}, and $\beta_{solvent}$.

The density (1.0124 g·cm^{-3}) of the reference PBS solvent and the density (1.0134 g·cm^{-3}) of the reference DMEM solvent at 293 K were determined with an automatic pycnometer (AccuPyc 1330; Shimadzu Corporation, Kyoto, Japan) installed at the Northeastern Industrial Research Center of Shiga Prefecture, Shiga, Japan. The scattering length density (9.962 μÅ^{-2}) of the reference PBS solvent and the scattering length density (9.433 μÅ^{-2}) of the reference DMEM solvent at 293 K were calculated from the above equation for $\beta_{solvent}$.

Standard statistical parameters and coefficients of determination (R^2) for the least-squares fit calculation have been reported elsewhere [40]; however, they are provided below because the description is important for this study. R^2 is given by

$$R^2 = 1 - \frac{\sum_{k=1}^{N_D}[\text{DSCS}(q)_{\text{data},k} - \text{DSCS}(q)_{\text{model},k}]^2}{\sum_{k=1}^{N_D}[\text{DSCS}(q)_{\text{data},k} - \text{DSCS}(q)_{\text{data,average}}]^2} \tag{S40}$$

where N_D and k are the total number of data points and the index of summation, respectively; $\text{DSCS}(q)_{\text{data},k}$ is the DSCS(q) value at the k-th data point; $\text{DSCS}(q)_{\text{data, average}}$ is the average of the DSCS(q) values; and $\text{DSCS}(q)_{\text{model},k}$ is the DSCS(q) value calculated from the best fit model to the SAXS data at the k-th data point. The R^2 coefficient of determination is a statistical measure of how well the regression curve approximates the real data points. An R^2 of 1.0 indicates that the regression curve perfectly fits the data[40].

In addition, a statistical test for goodness-of-fit was attempted. The chi-squared parameter χ^2 is given by

$$\chi^2 = \sum_{K=1}^{N_D} \frac{[\text{DSCS}(q)_{\text{data,k}} - \text{DSCS}(q)_{\text{model,k}}]^2}{\text{DSCS}(q)_{\text{model,k}}} \tag{S41}$$

The degrees of freedom (df) are listed in Tables S2–S9. P-values, $P(\chi^2)$, were calculated by using the functions of Microsoft Excel. The P-value is a statistical measure of how well a regression curve approximates the real data points. A $P(\chi^2)$ of 1.0 indicates that the regression curve perfectly fits the data.

The standard for determining a model was set as an R^2 coefficient of 0.997 or greater. An R^2 coefficient of 0.997 or greater also indicates a P (χ^2) of 1.0.

SAXS data analysis algorithms for the least-squares fit calculations for the models and the SAXS data were based on a simplex method (polytope method) and algorithms for numerical calculations (Integral calculation etc.) using a Microsoft Excel Macro[38-42].
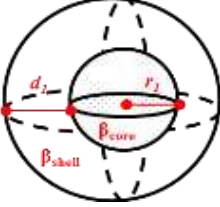
S4. Results
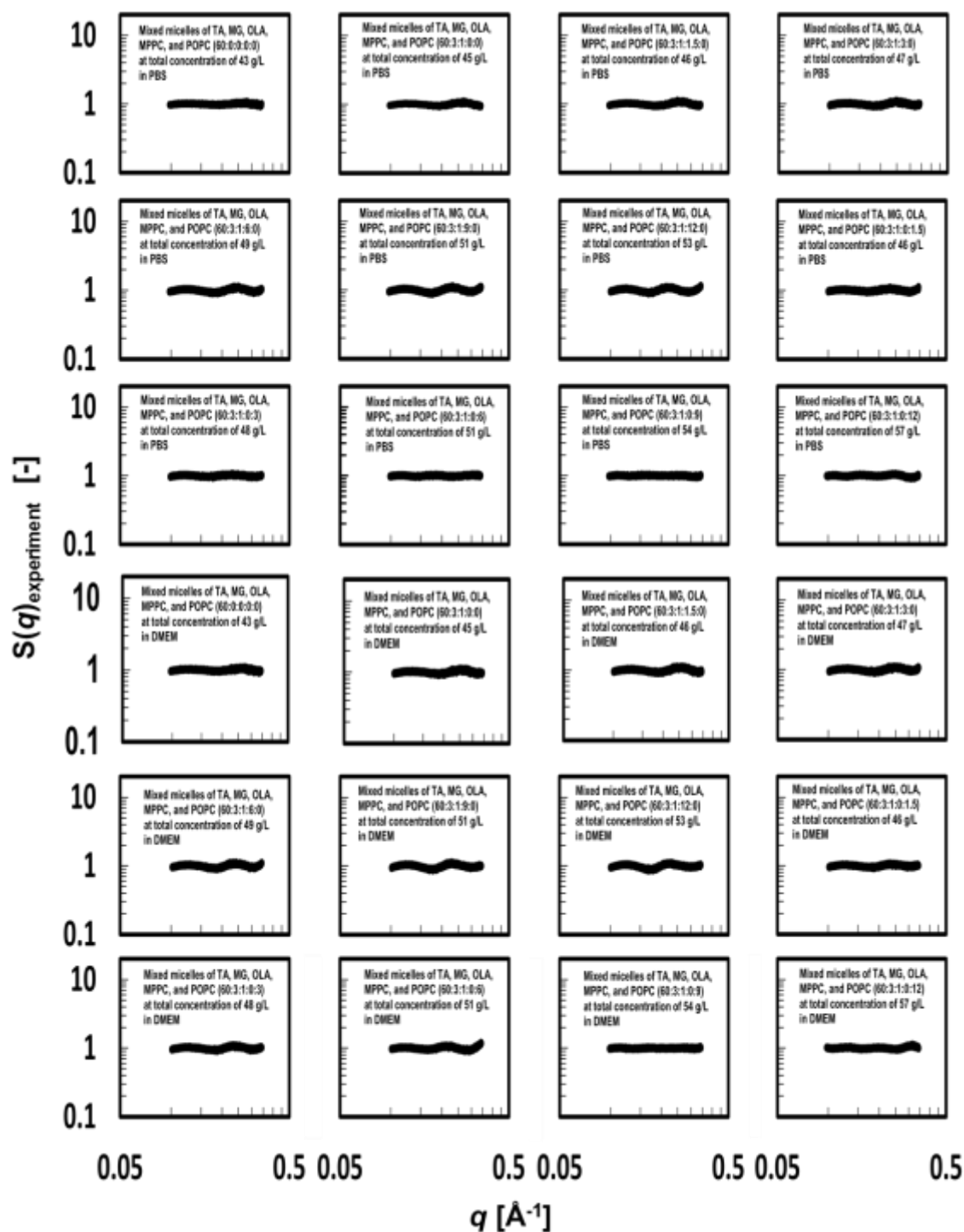
Figure S7 Experimental structure factors, $S(q)_{experiment}$ (black lines), were calculated from equation (S16) for mixed micelles of taurocholic acid (TA), 1-oleoyl-*rac*-glycerol (MG), oleic acid (OLA), and 1-palmitoyl-*sn*-glycero-3-phosphocholine (MPPC) or 1-palmitoyl-2-oleoyl-*sn*-glycero-3-phosphocholine (POPC) listed in Table 1, as prepared in phosphate-buffered saline (PBS) or Dulbecco's modified Eagle medium (DMEM).

Table S2 Shape parameters, coefficients of determination, and goodness-of-fit test parameters for core‑shell spherical mixed micelles of taurocholic acid (TA), 1-oleoyl-*rac*-glycerol (MG), and oleic acid (OLA) in phosphate-buffered saline (PBS).

Core–shell sphere
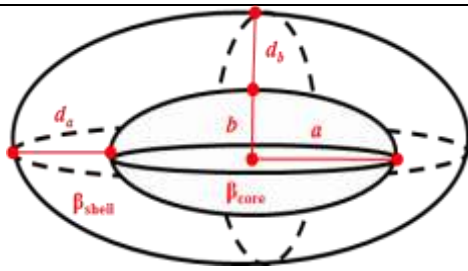
$n \pm SD$ (zÅ^{-3})	$70 \pm 1.4 \times 10^{-6}$	$54 \pm 7.4 \times 10^{-7}$
$r_1 \pm SD$ (Å)	$7.0 \pm 7.5 \times 10^{-8}$	$7.0 \pm 5.5 \times 10^{-8}$
$d_1 \pm SD$ (Å)	$15 \pm 7.5 \times 10^{-9}$	$17 \pm 1.1 \times 10^{-7}$
$(r_1 + d_1) \pm SD$ (Å)	$22 \pm 7.5 \times 10^{-8}$	$24 \pm 1.2 \times 10^{-7}$
$V_{\text{solute}} \pm SD$ (kÅ^3)	$43 \pm 7.6 \times 10^{-7}$	$54 \pm 8.3 \times 10^{-7}$
$\beta_{\text{core}} \pm SD$ (mÅ^{-2})	$0.9 \pm 1.3 \times 10^{-7}$	$3.1 \pm 1.4 \times 10^{-7}$
$\beta_{\text{shell}} \pm SD$ (μÅ^{-2})	$50 \pm 5.4 \times 10^{-6}$	$150 \pm 4.0 \times 10^{-6}$
$R^2 \pm SD$	$1.0 \pm 1.1 \times 10^{-16}$	$1.0 \pm 8.6 \times 10^{-17}$
$\chi^2 \pm SD$	$4.1 \pm 1.9 \times 10^{-7}$	$9.8 \pm 9.5 \times 10^{-7}$
df	589	589
$P(\chi^2)$	1.0	1.0

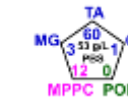*n,* the number density of the solute; SD, standard deviation; z (zepto-), 10^{-21}; V_{solute}, solute volume; R^2, coefficient of determination; χ^2, chi-squared parameter; *df*, degrees of freedom; $P(\chi^2)$, *P*-value.

Table S3 Shape parameters, coefficients of determination, and goodness-of-fit test parameters for core‑shell oblate ellipsoid mixed micelles of taurocholic acid (TA), 1-oleoyl-*rac*-glycerol (MG), oleic acid (OLA), and 1-palmitoyl-*sn*-glycero-3-phosphocholine (MPPC) in phosphate-buffered saline (PBS).

Core‑shell oblate ellipsoid

	TA MG 3 49 g/L 1 OLA 1.5 0 MPPC POPC	TA MG 3 47 g/L 1 OLA 3 0 MPPC POPC	TA MG 3 49 g/L 1 OLA 6 0 MPPC POPC	TA MG 3 51 g/L 1 OLA 9 0 MPPC POPC	TA MG 3 53 g/L 1 OLA 12 0 MPPC POPC
$n \pm SD$ (zÅ^{-3})	$41 \pm 5.9\times10^{-2}$	$32 \pm 3.4\times10^{-1}$	67 ± 1.0	$57 \pm 5.3\times10^{-2}$	65 ± 5.1
$a \pm SD$ (Å)	$7.3 \pm 6.2\times10^{-2}$	$7.4 \pm 6.6\times10^{-2}$	$7.6 \pm 3.6\times10^{-2}$	$7.8 \pm 2.1\times10^{-3}$	$7.7 \pm 1.5\times10^{-1}$
$d_a \pm SD$ (Å)	$18 \pm 1.2\times10^{-1}$	$18 \pm 1.4\times10^{-1}$	$21 \pm 1.0\times10^{-1}$	$23 \pm 4.0\times10^{-3}$	$26 \pm 8.7\times10^{-1}$
$b \pm SD$ (Å)	$5.8 \pm 1.9\times10^{-1}$	$6.9 \pm 2.4\times10^{-1}$	$5.7 \pm 1.3\times10^{-1}$	$5.7 \pm 5.4\times10^{-3}$	$4.4 \pm 7.3\times10^{-1}$
$d_b \pm SD$ (Å)	$19 \pm 3.2\times10^{-1}$	$22 \pm 3.4\times10^{-1}$	$12 \pm 1.6\times10^{-1}$	$13 \pm 1.2\times10^{-2}$	$12 \pm 4.1\times10^{-1}$
$V_{\text{solute}} \pm SD$ (kÅ^3)	65 ± 1.9	88 ± 2.6	$38 \pm 8.8\times10^{-1}$	$44 \pm 6.5\times10^{-2}$	40 ± 4.0
$\beta_{\text{core}} \pm SD$ (mÅ^{-2})	$1.7 \pm 5.7\times10^{-2}$	$1.0 \pm 3.6\times10^{-2}$	$1.5 \pm 2.3\times10^{-2}$	$9.8 \pm 7.1\times10^{-9}$	$9.7 \pm 2.4\times10^{-5}$
$\beta_{\text{shell}} \pm SD$ ($\mu\text{Å}^{-2}$)	69 ± 1.5	$46 \pm 8.3\times10^{-1}$	$77 \pm 7.5\times10^{-1}$	$10 \pm 4.0\times10^{-6}$	$10 \pm 2.1\times10^{-3}$
$R^2 \pm SD$	$1.0 \pm 4.5\times10^{-6}$	$1.0 \pm 2.0\times10^{-6}$	$1.0 \pm 3.0\times10^{-6}$	$1.0 \pm 1.4\times10^{-7}$	$1.0 \pm 1.3\times10^{-4}$
$\chi^2 \pm SD$	$12 \pm 2.4\times10^{-1}$	$12 \pm 1.9\times10^{-1}$	$19.5 \pm 3.4\times10^{-1}$	$24.6 \pm 3.4\times10^{-3}$	25.8 ± 3.9
df	589	584	589	589	584
$P(\chi^2)$	1.0	1.0	1.0	1.0	1.0

n, the number density of the solute; SD, standard deviation; z (zepto-), 10^{-21}; V_{solute}, solute volume; R^2, coefficient of determination; χ^2, chi-squared parameter; *df*, the degrees of freedom; $P(\chi^2)$, *P*-value.

Table S4 Shape parameters, coefficients of determination, and goodness-of-fit test parameters for core‑shell oblate ellipsoid mixed micelles of taurocholic acid (TA), 1-oleoyl-*rac*-glycerol (MG), oleic acid (OLA), and 1-palmitoyl-2-oleoyl-*sn*-glycero-3-phosphocholine (POPC) in phosphate-buffered saline (PBS).

Core‑shell oblate ellipsoid

	MG TA OLA MPPC POPC (3.48 gL-1 PBS) 0 1.5	MG TA OLA MPPC POPC (3.48 gL-1 PBS) 0 3	MG TA OLA MPPC POPC (3.51 gL-1 PBS) 0 6
$n \pm$ SD (zÅ^{-3})	$16 \pm 4.8 \times 10^{-2}$	$38 \pm 3.6 \times 10^{-1}$	$55 \pm 4.1 \times 10^{-1}$
$a \pm$ SD (Å)	$8.2 \pm 6.1 \times 10^{-3}$	$5.7 \pm 1.8 \times 10^{-2}$	$8.6 \pm 1.1 \times 10^{-2}$
$d_a \pm$ SD (Å)	$21 \pm 3.9 \times 10^{-2}$	$18 \pm 1.1 \times 10^{-2}$	$34 \pm 2.1 \times 10^{-2}$
$b \pm$ SD (Å)	$4.9 \pm 4.0 \times 10^{-2}$	$17 \pm 1.5 \times 10^{-1}$	$1.7 \pm 1.2 \times 10^{-2}$
$d_b \pm$ SD (Å)	$27 \pm 9.4 \times 10^{-2}$	$18 \pm 1.8 \times 10^{-1}$	$9.5 \pm 3.9 \times 10^{-2}$
$V_{\text{solute}} \pm$ SD (kÅ^3)	$124 \pm 8.2 \times 10^{-1}$	125 ± 1.7	$22 \pm 1.6 \times 10^{-1}$
$\beta_{\text{core}} \pm$ SD (mÅ^{-2})	$2.7 \pm 2.3 \times 10^{-2}$	$1.7 \pm 8.4 \times 10^{-3}$	$0.95 \pm 1.8 \times 10^{-3}$
$\beta_{\text{shell}} \pm$ SD (µÅ^{-2})	$65 \pm 2.1 \times 10^{-1}$	$100 \pm 5.5 \times 10^{-1}$	$25 \pm 5.8 \times 10^{-2}$
$R^2 \pm$ SD	$1.0 \pm 8.5 \times 10^{-7}$	$1.0 \pm 2.9 \times 10^{-6}$	$1.0 \pm 3.7 \times 10^{-6}$
$\chi^2 \pm$ SD	$7.7 \pm 6.4 \times 10^{-2}$	$4.8 \pm 1.1 \times 10^{-1}$	$3.0 \pm 4.2 \times 10^{-2}$
df	584	586	578
$P\ (\chi^2)$	1.0	1.0	1.0

n, the number density of the solute; SD, standard deviation; z (zepto-), 10^{-21}; V_{solute}, solute volume; R^2, coefficient of determination; χ^2, chi-squared parameter; *df*, the degrees of freedom; $P\ (\chi^2)$, *P*-value.
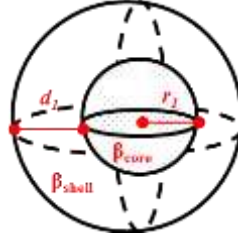
Table S5 Shape parameters, coefficients of determination, and goodness-of-fit test parameters for core‑shell cylindrical mixed micelles of taurocholic acid (TA), 1-oleoyl-*rac*-glycerol(MG), oleic acid (OLA), and 1-palmitoyl-2-oleoyl-*sn*-glycero-3-phosphocholine (POPC) in phosphate-buffered saline (PBS).

Core‑shell cylinder
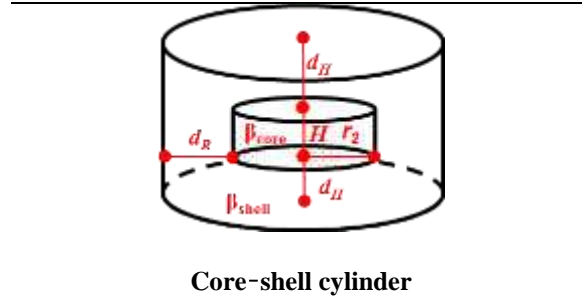
$n \pm$ SD (zÅ^{-3})	$7.2 \pm 1.1 \times 10^{-1}$	$6.3 \pm 5.8 \times 10^{-3}$
$r_2 \pm$ SD (Å)	$9.9 \pm 9.3 \times 10^{-2}$	$10 \pm 9.5 \times 10^{-4}$
$d_R \pm$ SD (Å)	$23 \pm 1.6 \times 10^{-1}$	$31 \pm 5.0 \times 10^{-3}$
$H \pm$ SD (Å)	$2.0 \pm 3.4 \times 10^{-2}$	$2.1 \pm 1.9 \times 10^{-3}$
$d_H \pm$ SD (Å)	$38 \pm 3.0 \times 10^{-1}$	$34 \pm 8.4 \times 10^{-3}$
$V_{solute} \pm$ SD (kÅ^3)	276 ± 11	$373 \pm 7.3 \times 10^{-1}$
$\beta_{core} \pm$ SD (mÅ^{-2})	$5.5 \pm 4.2 \times 10^{-2}$	$5.7 \pm 5.4 \times 10^{-3}$
$\beta_{shell} \pm$ SD (µÅ^{-2})	$38 \pm 2.6 \times 10^{-1}$	$40 \pm 2.1 \times 10^{-2}$
$R^2 \pm$ SD	$1.0 \pm 2.9 \times 10^{-4}$	$1.0 \pm 2.3 \times 10^{-7}$
$\chi^2 \pm$ SD	2.8 ± 1.6	$9.0 \pm 7.4 \times 10^{-3}$
df	589	589
$P(\chi^2)$	1.0	1.0

n, the number density of the solute; SD, standard deviation; z (zepto-), 10^{-21}; V_{solute}, solute volume; R^2, coefficient of determination; χ^2, chi-squared parameter; *df*, the degrees of freedom; $P(\chi^2)$, *P*-value.

Table S6   Shape parameters, coefficients of determination, and goodness-of-fit test parameters for core‑shell spherical mixed micelles of taurocholic acid (TA), 1-oleoyl-*rac*-glycerol (MG), and oleic acid (OLA) in Dulbecco's modified Eagle medium (DMEM).
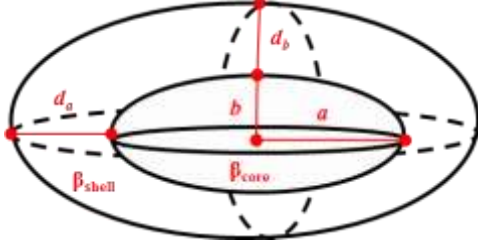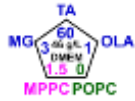

Core–shell sphere

	MG 0.43 pL TA 60 OLA 0 DMEM 0 MPPC 0 POPC	MG 3 pL TA 60 OLA 1 DMEM 0 MPPC 0 POPC
$n \pm$ SD (zÅ^{-3})	$70 \pm 1.0 \times 10^{-6}$	$53 \pm 1.1 \times 10^{-6}$
$r_1 \pm$ SD (Å)	$7.0 \pm 4.5 \times 10^{-8}$	$7.3 \pm 1.6 \times 10^{-7}$
$d_1 \pm$ SD (Å)	$15 \pm 9.4 \times 10^{-9}$	$17 \pm 8.4 \times 10^{-8}$
$(r_1 + d_1) \pm$ SD (Å)	$22 \pm 4.6 \times 10^{-8}$	$24 \pm 1.8 \times 10^{-7}$
$V_{\text{solute}} \pm$ SD (kÅ^3)	$50 \pm 2.8 \times 10^{-7}$	$58 \pm 1.3 \times 10^{-6}$
$\beta_{\text{core}} \pm$ SD (mÅ^{-2})	$1.3 \pm 1.9 \times 10^{-8}$	$0.3 \pm 7.0 \times 10^{-8}$
$\beta_{\text{shell}} \pm$ SD ($\mu\text{Å}^{-2}$)	$74 \pm 1.1 \times 10^{-6}$	$25 \pm 3.4 \times 10^{-6}$
$R^2 \pm$ SD	$1.0 \pm 1.1 \times 10^{-16}$	$1.0 \pm 1.3 \times 10^{-6}$
$\chi^2 \pm$ SD	$7.0 \pm 5.0 \times 10^{-7}$	$11 \pm 9.1 \times 10^{-7}$
df	589	583
$P (\chi^2)$	1.0	1.0

n, the number density of the solute; SD, standard deviation; z (zepto-), 10^{-21}; V_{solute}, the volume of the solute; R^2, coefficient of determination; χ^2, chi-squared parameter; *df*, the degrees of freedom; $P (\chi^2)$, *P*-value.

Table S7 Shape parameters, coefficients of determination, and goodness-of-fit test parameters for core‑shell oblate ellipsoid mixed micelles of taurocholic acid (TA), 1-oleoyl-*rac*-glycerol (MG), oleic acid (OLA), and 1-palmitoyl-*sn*-glycero-3-phosphocholine (MPPC) in Dulbecco's modified Eagle medium (DMEM).

Core‑shell oblate ellipsoid

	TA/MG/OLA/MPPC/POPC 1.5 g L⁻¹ DMEM	TA/MG/OLA/MPPC/POPC 3 g L⁻¹ DMEM	TA/MG/OLA/MPPC/POPC 6 g L⁻¹ DMEM	TA/MG/OLA/MPPC/POPC 9 g L⁻¹ DMEM	TA/MG/OLA/MPPC/POPC 12 g L⁻¹ DMEM
$n \pm$ SD (zÅ^{-3})	52 ± 2.4	$41 \pm 1.1\times10^{-1}$	$36 \pm 9.6\times10^{-1}$	$40 \pm 1.9\times10^{-1}$	$32 \pm 5.1\times10^{-2}$
$a \pm$ SD (Å)	$7.0 \pm 4.7\times10^{-2}$	$7.6 \pm 6.7\times10^{-3}$	$9.3 \pm 1.0\times10^{-1}$	$7.3 \pm 2.4\times10^{-2}$	$8.33 \pm 7.1\times10^{-3}$
$d_a \pm$ SD (Å)	$19 \pm 4.0\times10^{-1}$	$19 \pm 1.8\times10^{-1}$	$17 \pm 7.1\times10^{-1}$	$26 \pm 4.3\times10^{-2}$	$26 \pm 2.5\times10^{-2}$
$b \pm$ SD (Å)	$7.1 \pm 5.2\times10^{-1}$	$7.7 \pm 8.1\times10^{-2}$	$3.7 \pm 1.5\times10^{-1}$	$3.2 \pm 3.4\times10^{-2}$	$2.2 \pm 3.4\times10^{-3}$
$d_b \pm$ SD (Å)	$14 \pm 5.5\times10^{-1}$	$18 \pm 3.4\times10^{-1}$	26 ± 1.4	$17 \pm 4.2\times10^{-2}$	$20 \pm 2.6\times10^{-2}$
$V_{\text{solute}} \pm$ SD (kÅ^3)	51 ± 3.7	72 ± 2.0	99 ± 9.9	$56 \pm 3.2\times10^{-1}$	$71 \pm 1.8\times10^{-1}$
$\beta_{\text{core}} \pm$ SD (mÅ^{-2})	$2.2 \pm 2.0\times10^{-1}$	$1.0 \pm 6.0\times10^{-3}$	$1.9 \pm 1.2\times10^{-1}$	$10 \pm 6.2\times10^{-5}$	$1.6 \pm 1.5\times10^{-3}$
$\beta_{\text{shell}} \pm$ SD (µÅ^{-2})	112 ± 6.9	$56 \pm 6.8\times10^{-2}$	70 ± 5.7	$9.5 \pm 1.3\times10^{-3}$	$37 \pm 1.5\times10^{-2}$
$R^2 \pm$ SD	$1.0 \pm 4.1\times10^{-5}$	$1.0 \pm 3.1\times10^{-6}$	$1.0 \pm 6.3\times10^{-5}$	$1.0 \pm 6.6\times10^{-6}$	$1.0 \pm 5.8\times10^{-7}$
$\chi^2 \pm$ SD	16 ± 1.7	$13 \pm 6.8\times10^{-2}$	$17 \pm 8.6\times10^{-1}$	$23 \pm 2.3\times10^{-1}$	$23 \pm 1.4\times10^{-1}$
df	583	582	580	582	583
$P (\chi^2)$	1.0	1.0	1.0	1.0	1.0

n, the number density of the solute; SD, standard deviation; z (zepto-), 10^{-21}; V_{solute}, the volume of the solute; R^2, coefficient of determination; χ^2, chi-squared parameter; *df*, the degrees of freedom; $P (\chi^2)$, *P*-value.
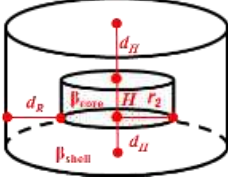
Table S8   Shape parameters, coefficients of determination, and goodness-of-fit test parameters for core‑shell oblate ellipsoid mixed micelles of taurocholic acid (TA), 1-oleoyl-*rac*-glycerol (MG), oleic acid (OLA), and 1-palmitoyl-2-oleoyl-*sn*-glycero-3-phosphocholine (POPC) in Dulbecco's modified Eagle medium (DMEM).
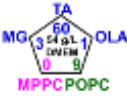

Core‑shell oblate ellipsoid

	TA / MG / OLA / MPPC / POPC (80, 3 46 g L 1, DMEM, 0 1.5)	TA / MG / OLA / MPPC / POPC (80, 3 48 g L 1, DMEM, 0 3)	TA / MG / OLA / MPPC / POPC (80, 3 51 pL 1, DMEM, 0 6)
$n \pm$ SD (zÅ^{-3})	$51 \pm 5.3 \times 10^{-2}$	52 ± 4.4	$43 \pm 8.9 \times 10^{-3}$
$a \pm$ SD (Å)	$6.8 \pm 7.6 \times 10^{-3}$	$7.3 \pm 1.1 \times 10^{-1}$	$5.4 \pm 6.3 \times 10^{-4}$
$d_a \pm$ SD (Å)	$15 \pm 2.3 \times 10^{-2}$	$23 \pm 5.2 \times 10^{-1}$	$29 \pm 1.5 \times 10^{-3}$
$b \pm$ SD (Å)	$6.3 \pm 3.0 \times 10^{-2}$	$5.8 \pm 6.5 \times 10^{-1}$	$10 \pm 9.6 \times 10^{-4}$
$d_b \pm$ SD (Å)	$29 \pm 6.4 \times 10^{-2}$	$13 \pm 5.1 \times 10^{-1}$	$6.2 \pm 1.7 \times 10^{-3}$
$V_{solute} \pm$ SD (kÅ^3)	$112 \pm 4.7 \times 10^{-1}$	43 ± 3.9	$38 \pm 9.1 \times 10^{-3}$
$\beta_{core} \pm$ SD (mÅ^{-2})	$1.2 \pm 8.0 \times 10^{-3}$	$0.19 \pm 5.6 \times 10^{-3}$	$0.10 \pm 2.9 \times 10^{-5}$
$\beta_{shell} \pm$ SD (µÅ^{-2})	$54 \pm 2.5 \times 10^{-1}$	$17 \pm 1.9 \times 10^{-1}$	$13 \pm 4.1 \times 10^{-4}$
$R^2 \pm$ SD	$1.0 \pm 2.8 \times 10^{-6}$	$1.0 \pm 8.2 \times 10^{-5}$	$1.0 \pm 4.2 \times 10^{-9}$
$\chi^2 \pm$ SD	$9.4 \pm 1.0 \times 10^{-1}$	$13 \pm 4.7 \times 10^{-1}$	$16 \pm 2.4 \times 10^{-3}$
df	581	581	582
$P(\chi^2)$	1.0	1.0	1.0

n, the number density of the solute; SD, standard deviation; z (zepto-), 10^{-21}; V_{solute}, the volume of the solute; R^2, coefficient of determination; χ^2, chi-squared parameter; *df*, the degrees of freedom; $P(\chi^2)$, P-value.

Table S9 Shape parameters, coefficients of determination, and goodness-of-fit test parameters for core‑shell cylindrical mixed micelles of taurocholic acid (TA), 1-oleoyl-*rac*-glycerol (MG), oleic acid (OLA), and 1-palmitoyl-2-oleoyl-*sn*-glycero-3-phosphocholine (POPC) in Dulbecco's modified Eagle medium (DMEM).

Core‑shell cylinder

	TA/MG/OLA/POPC/MPPC (…9)	TA/MG/OLA/POPC/MPPC (…12)
$n \pm$ SD (zÅ^{-3})	$8.7 \pm 1.4 \times 10^{-2}$	$7.0 \pm 4.2 \times 10^{-3}$
$r_2 \pm$ SD (Å)	$9.9 \pm 4.8 \times 10^{-3}$	$11 \pm 1.4 \times 10^{-2}$
$d_R \pm$ SD (Å)	$22 \pm 9.6 \times 10^{-3}$	$30 \pm 1.7 \times 10^{-1}$
$H \pm$ SD (Å)	$3.6 \pm 5.5 \times 10^{-3}$	$2.2 \pm 6.6 \times 10^{-4}$
$d_H \pm$ SD (Å)	$37 \pm 3.7 \times 10^{-3}$	$33 \pm 2.8 \times 10^{-1}$
$V_{\text{solute}} \pm$ SD (kÅ^3)	247 ± 1.3	349 ± 6.7
$\beta_{\text{core}} \pm$ SD (mÅ^{-2})	$2.4 \pm 4.1 \times 10^{-3}$	$4.1 \pm 1.1 \times 10^{-2}$
$\beta_{\text{shell}} \pm$ SD (μÅ^{-2})	$34 \pm 1.5 \times 10^{-2}$	$35 \pm 4.3 \times 10^{-2}$
$R^2 \pm$ SD	$1.0 \pm 2.8 \times 10^{-6}$	$1.0 \pm 2.7 \times 10^{-5}$
$\chi^2 \pm$ SD	$1.4 \pm 1.1 \times 10^{-2}$	$8.7 \pm 2.6 \times 10^{-1}$
df	587	589
P (χ^2)	1.0	1.0

n, the number density of the solute; SD, standard deviation; z (zepto-), 10^{-21}; V_{solute}, the volume of the solute; R^2, coefficient of determination; χ^2, chi-squared parameter; *df*, the degrees of freedom; P (χ^2), *P*-value.